Title: Climate drives spatial variation in Zika epidemics in Latin America

Mallory Harris[1], Jamie M. Caldwell[2*], Erin A. Mordecai[2]

1. Odum School of Ecology, University of Georgia, 140 E Green St, Athens, GA 30602
2. Biology Department, Stanford University, 371 Serra Mall, Stanford, CA, USA

* contact: jcaldwel@stanford.edu

Keywords: Zika, force of infection, tSIR

Abstract

Between 2015 and 2017, Zika virus spread rapidly through populations in the Americas with no prior exposure to the disease. Here, we estimated force of infection for Zika over time and across provinces in Latin America using a time-varying Susceptible Infectious Recovered model. Climate factors explained less than 1% of the variation in force of infection over time, suggesting that week to week transmission within provinces may be too stochastic to predict. By contrast, climate and population factors explained 36-90% of variation in Zika presence and intensity among provinces. While humidity and temperature were the most important climate predictors of where Zika transmission occurred, rainfall, temperature range, and mean temperature were the best predictors of Zika intensity and burden, given that Zika was present. Surprisingly, force of infection was greatest in locations with temperatures near 24°C, much lower than previous estimates from mechanistic models, potentially suggesting that existing vector control programs and/or prior exposure to other mosquito-borne diseases may have limited transmission in locations most suitable for *Aedes aegypti*, the main vector of Zika, dengue, and chikungunya viruses in Latin America.

Introduction

The emergence and re-emergence of mosquito-borne diseases presents a global public health concern, yet trends in mosquito-borne disease transmission are hard to predict because they are influenced by the underlying immunity in the population, which is usually unknown [1–3]. The emergence and spread of Zika virus through Latin America in a population with no prior exposure or immunity to the disease provides an opportunity to characterize relationships between the environment, populations, and disease transmission without the confounding effects of pre-existing immunity (although cross-reactivity between dengue antibodies and Zika virus may provide some protection) [4]. Between 2015 and 2017, Zika rapidly spread to 51 countries and territories in the Americas, with over 800,000 cases reported [5]. Here, we quantified the force of infection for Zika and studied factors that contributed to variation in transmission across time and space as Zika emerged.

Force of infection, or the per capita rate at which susceptible individuals contract an infection, can be used to compare disease transmission over the course of an outbreak and across geographic regions [2,6]. Force of infection estimates can account for variation in the number of immune individuals and entomological factors that influence the time it takes for mosquito-borne diseases to be transmitted [2,6]. It can take up to several weeks for mosquitoes to spread diseases because transmission requires a mosquito to bite an infectious person, the pathogen to replicate and disseminate in the mosquito (the extrinsic incubation period), and the mosquito to bite and infect a susceptible person [2,7–9]. Force of infection can be calculated over time to study how transmission rate changes over the course of an outbreak and to compare outbreaks of the same disease in different places [2,6,10–12].

The progression of an epidemic can be characterized and compared through measures of burden, intensity, and transmission rate [13,14]. We can quantitatively differentiate between epidemics with sharp peaks in case incidence that quickly burn through the susceptible population and more sustained, low-level transmission [6,15,16]. Instances when high case incidence coincides with a low force of infection may indicate the presence of imported cases [17]. Each of these epidemic metrics may be affected to a different extent by climate and population factors, in addition to country and province-level features like existing transportation infrastructure and vector control resources [9,18–20]. Additionally, conditions that enable the establishment of a disease may differ from those that drive higher epidemic intensity following establishment [21].

Climate is a key determinant for whether mosquito-borne disease transmission can occur and the intensity of outbreaks because of its effects on vector dynamics. The primary vector of Zika in Latin America is *Aedes aegypti*, which also spreads chikungunya and dengue viruses [22]. Disease transmission can only occur if climate conditions are suitable for pathogen and vector survival and reproduction, while the intensity of transmission may be affected by how close humidity, temperature, and rainfall are to optimal climate conditions for vector and pathogen performance [2,9,23–28]. Humidity is positively associated with mosquito survival [24]. Temperature influences mosquito fecundity, development, and survival, as well as factors contributing directly to transmission, including the extrinsic incubation period and mosquito biting rate [9,25,28–30]. These thermal responses are nonlinear with optimal disease transmission expected at 29°C for viruses transmitted by *A. aegypti* based on mechanistic models parameterized from laboratory experiments [26,31]. Mosquitoes require water to complete their life cycle and breed, but the relationship between mosquito abundance and rainfall is variable

[32–38]. The most notable reasons for this varying relationship are associated with extreme conditions, such as heavy rainfall that can kill and wash away larvae [39,40], and drought, which in certain regions promotes humans to store water in open containers that serve as breeding habitats [37,38]. Understanding how climate drives the emergence and intensity of Zika will be important for identifying regions where the disease is likely to become endemic, and, more generally, for predicting the potential trajectories of similar mosquito-borne diseases that could emerge and re-emerge in the future, such as o'nyong nyong, Mayaro, and yellow fever [1,20,41–43].

In this study, we estimated weekly force of infection for Zika from human case reports across Latin America to examine the role of climate in driving the emergence and intensity of the 2015 to 2017 outbreak. Specifically, we use the models to ask how climate and population variation affect (1) when and where epidemics occur, (2) epidemic dynamics over time, and (3) geographic variation in the intensity of epidemics. We use disease case reports and force of infection estimates in two modeling frameworks. First, we examine variation in force of infection over time within provinces to understand how strongly climate predicts the probability of local transmission and the intensity of transmission. Then, we examine spatial variation in several epidemic metrics, including total human cases and force of infection, to understand how climate and population factors shape epidemics geographically.

Materials and Methods

Epidemiological Data

To investigate Zika transmission dynamics over time and space in Latin America, we downloaded and preprocessed publicly available human case data. We used weekly suspected

113 and confirmed Zika cases per province between November 2015 and November 2017 for
114 countries in Latin America from the Centers for Disease Control and Prevention (CDC) Zika
115 Data Repository, which includes Epidemiological Bulletins provided by each country's ministry
116 of health [44].We excluded provinces with fewer than ten weeks of case reporting, fewer than
117 ten cases total, or irregular reporting intervals, because those provinces provided insufficient data
118 to observe meaningful trends in transmission. For the remaining provinces, we temporally
119 interpolated case data for weeks with missing data and reporting errors by averaging cases from
120 the weeks immediately preceding and following these intervals.
121
122 *Weather Data*
123 To investigate the effects of climate on Zika transmission, we downloaded weather data
124 and calculated climate metrics with time lags relevant to diseases spread by the *Aedes aegypti*
125 vector. We downloaded daily mean relative humidity, total precipitation, and mean, minimum,
126 and maximum temperatures from Weather Underground [45]. For each province, we used the
127 weather station nearest to the province's centroid that had the most complete climate record in
128 the timespan corresponding to the case data. We then discarded provinces that had no nearby
129 weather station reporting in the desired time period, and further excluded weeks with mean
130 temperatures outside of the range of 0-40°C and rainfall values exceeding 250mm. To investigate
131 the spatiotemporal dynamics of transmission, we calculated lagged climate metrics to account for
132 the delay at which humidity, temperature, and rainfall influence transmission. Specifically, we
133 calculated humidity, mean temperature, and temperature range (difference between the
134 maximum and minimum temperatures observed) over a three-week period, lagged by six weeks
135 from the week of case reporting (i.e., nine to six weeks prior) [21,46,47]. Similarly, we

136 calculated the cumulative rainfall over a six-week period, lagged by three weeks from the week
137 of case reporting (i.e., nine to three weeks prior) [48,49]. To compare differences in overall
138 epidemic characteristics (e.g., total number of cases, average force of infection; Table 1) among
139 provinces, we also calculated province-level mean humidity, mean temperature, temperature
140 range, and cumulative rainfall over the biologically relevant time lag described above.
141
142 *tSIR Model*
143 We estimated weekly force of infection by fitting time-varying Susceptible Infectious
144 Recovered (tSIR) models to the human case data [44]. We assumed a static population size
145 because the human population did not change significantly over the course of the epidemic, and
146 we assumed that Zika was introduced to a fully susceptible population since it had never been
147 documented before in this region. Therefore, we set the initial susceptible population (S_0) as the
148 most recent estimate of population (N) available from *City Population* [50] as of June 2017, and
149 modeled the susceptible population following Zika introduction as $S_t = S_{t-1} - I_t$. We followed
150 the modification of the tSIR model for vector-borne diseases developed by Perkins et al 2015 for
151 chikungunya transmission because of similarities in the transmission ecology of their shared
152 vector [2,36]. Using the infectious periods derived for chikungunya, we assumed that individuals
153 remained infectious for five days, but that secondary infections could arise from primary cases
154 reported several weeks prior because the time between cases is dependent on a mosquito vector
155 [51]. We calculated the effective number of infectious individuals (I_t') as a weighted sum of
156 infectious individuals (I_{t-n}) within a serial interval as:

$$I_t' = \sum_{n=1}^{k} \omega_n I_{t-n} \quad (1)$$

157 We used the same five-week serial interval ($k = 5$) and weighting distribution ($\omega_{1,\ldots,5} = 0.011$,
158 0.187, 0.432, 0.287, and 0.083) as the Perkins et al 2015 model for chikungunya transmission
159 [2,52]. Individuals entered the recovered class after the five-week serial interval. We fit tSIR
160 models to case data for each province to calculate time-varying force of infection parameters
161 ($\beta_t{}'s$):

$$I_t = \beta_t \frac{{I_t'}^{\alpha}}{N} S_{t-1} \tag{2}$$

162 Here, the mixing parameter α indicates homogeneous frequency-dependent contact rate between
163 cases in each province. By rearranging equation 2 into a linear regression, we solved for β_t and
164 α using the following equation:

$$\ln(I_t) - \ln(N) - \ln(S_{t-1}) = \ln(\beta_t) + \alpha \ln(I_t') \tag{3}$$

165

166 *Spatiotemporal Model*

167 We investigated how strongly climate predicts the probability of local transmission and
168 the intensity of transmission by regressing weekly force of infection with biologically relevant
169 lagged climate factors. Since the force of infection (β_t) values were inflated between zero and
170 one, which indicates sporadic transmission, we fit a two-step hurdle model that first predicts the
171 probability that β_t will exceed one in a given week and province (i.e., presence/absence), and
172 then predicts the magnitude of β_t (i.e., intensity), given that β_t exceeds one. We performed
173 stepwise model selection using bidirectional elimination, selecting the best fit models for both
174 steps of the hurdle model as those with the lowest Akaike information criterion (AIC). To
175 account for variation among provinces within countries and among countries, both models
176 incorporated nested fixed effects of province within country. To capture nonlinear relationships
177 between force of infection and temperature, we included a squared term for mean temperature

178 [2,9,31]. To assess the goodness of fit of the model to data, we calculated pseudo R^2 for these
179 generalized linear mixed-effects models using the methods outlined by Nakagawa and Schielzeth
180 [53].
181
182 *Spatial Models*
183 To examine the factors that drove broad-scale geographic differences in Zika
184 transmission, we used linear regressions to compare epidemic metrics with climate and
185 population factors. The response variables included epidemic metrics based on incidence and
186 force of infection, where each response variable was aggregated to a single value per province
187 (Table 1; Figure 1). To account for additional variation among countries beyond climate and
188 population factors, we included country as a fixed effect. For the population factor, used the
189 number of people living in the largest city in each province based on census results and official
190 estimates of the population of each province's largest city and total population as of June 2017
191 downloaded from *City Population* (S1) [50]. For each spatial model, we performed stepwise
192 model selection using bidirectional elimination, selecting the best fit models as those with the
193 lowest AIC and calculated pseudo R^2 using Cragg, Uhler, and Nagelkerke's method for fixed
194 effect models [54,55]. All regressions were conducted in R statistical software version 3.4.3
195 using the glm function in the base package.
196
197 **Results**:
198 *Epidemiological Data*
199 The duration and burden of Zika transmission and timing of epidemic peaks varied
200 considerably both between and within countries (Figure 2). Within the countries included in this

study, Zika emerged earliest in El Salvador in November of 2015, and latest in Colombia, with the first Colombian case report occurring almost one year later in January of 2016 (Figure 2A). Force of infection ranged from 0 to 132 per 100,000 people per week. In all countries there were weeks with no local transmission (force of infection values below one), but high case incidence resulting from imported cases. All of the countries included in our analyses had at least one province with and one province without local transmission (Figure 2B).

Spatiotemporal Model

The spatiotemporal hurdle model indicated that different climate factors were associated with the presence of local transmission in a given province and week compared with the magnitude of force of infection, but most of the variation was explained by non-climate factors associated with province (Table 2). The best fit model for the presence of local transmission included positive linear relationships with maximum temperature and humidity and explained 15% of the variance in week to week transmission within provinces (conditional pseudo R^2=0.15). However, maximum temperature and humidity accounted for only 2% of the total variation (marginal pseudo R^2 = 0.02). The best fit model for the intensity of the force of infection included a slight positive linear relationship with rainfall, a negative linear relationship with temperature range, and a negative quadratic relationship with mean temperature and explained 55% of the variance (conditional pseudo R^2 = 0.55). However, rainfall, mean temperature, and temperature range only accounted for 4% of the total variation (marginal pseudo R^2 = 0.04).

Spatial Models

The spatial models indicated that geographic variation in epidemics was driven by temperature, rainfall, humidity, and human population sizes. There was considerable geographic variation in Zika presence and intensity within and among countries in Latin America (e.g., Figure 3). We found a positive relationship between the presence of local transmission and humidity and population of the province's largest city (Figure 4A). In provinces that had local transmission, we found a unimodal relationship with mean temperature (positive linear effect of mean temperature and negative quadratic effect of mean temperature; Figure 4A) with the peak in average force of infection at a mean temperature of 24°C (Figure 5), and a positive linear relationship with rainfall (Figure 4). Temperature range had a slight negative relationship with cumulative cases and maximum force of infection (Figure 4A). All the epidemic metrics were positively associated with the population of the province's largest city (Figure 4A). Epidemic metrics were more similar among provinces within countries than among countries: El Salvador and Guatemala had the highest average and cumulative cases and average and maximum force of infection values, while Mexico consistently had the lowest values for the same metrics (Figure 4B). The spatial models for local transmission and maximum and average force of infection explained 90%, 83%, and 79% of variation among provinces, respectively, based on pseudo R^2 values. The spatial models for cumulative cases and average weekly cases explained less variance among provinces, explaining only 39% and 36% of the variation respectively, based on pseudo R^2 values.

247 **Discussion:**

248 Climate was a strong driver of geographic variation in Zika epidemics, with different
249 climate factors influencing where local transmission occurred compared with the intensity of
250 transmission. Understanding how climate drives different epidemic metrics is valuable for
251 preparing for and responding to outbreaks. For example, the infrastructure and resources needed
252 to respond to a large outbreak that spreads rapidly through the population, like what occurred in
253 the Dominican Republic and El Salvador, are very different from what is needed to respond to an
254 outbreak that affects fewer people at one time but lasts many months, as in Colombia and
255 Guatemala. Mean relative humidity and temperature were key determinants for whether local
256 transmission occurred, and these two factors could be used to determine regional likelihood for
257 future *Aedes aegypti* transmitted diseases. Temperature range was the major climate driver that
258 differentiated more intense outbreaks from less intense outbreaks, indicated by drivers of high
259 cumulative cases and maximum force of infection compared with drivers of average cases and
260 average force of infection (Figure 4A). This result suggests that provinces with greater
261 temperature ranges may be associated with lower force of infection due to longer periods of time
262 with unsuitable temperatures for vector growth and pathogen transmission.

263 Although climate strongly influenced spatial variation in Zika epidemic metrics, climate
264 was not a strong predictor of Zika epidemic dynamics through time [23,30,39]. We hypothesize
265 that week to week variation in transmission within provinces may be too stochastic to predict
266 based on climate alone. For many of the provinces included in this study, climate rarely
267 exceeded suitable conditions for transmission, potentially indicating that given suitable climate
268 conditions, non-climate factors such as reporting protocols, underlying immunity, transportation,

269 and infrastructure may generate stochasticity that drives local temporal trends in Zika
270 transmission.

271 A surprising result of this study was the mismatch between the theoretically and
272 empirically derived optimal temperature for Zika transmission and the temperature we found to
273 correspond with maximum force of infection during the 2015 to 2017 epidemic. In previous
274 studies, both mechanistic R_0 models and laboratory experiments indicated that 29°C is optimal
275 for Zika transmission [27,32]. However, our study demonstrated that the most intense Zika
276 epidemics occurred in provinces with mean temperatures at 24°C. There are several possible
277 hypotheses that could explain this discrepancy, including that: 1) provinces with average
278 temperatures around 29°C already implement vector control; 2) people may have acquired cross-
279 immunity from exposure to other arboviruses [26,56,57]; 3) given suitable temperature for
280 transmission, other factors that can covary with temperature such as land use, urbanization, and
281 socioeconomics may be more important drivers of big epidemics [31]; and/or 4) transmission
282 plateaus due to burn-out of susceptible people in large epidemics [58]. Even when accounting for
283 a declining susceptible population in a tSIR model framework, it is possible for force of infection
284 to become decoupled from climate due to internal disease dynamics (i.e., regardless of how
285 suitable the temperature is, there will be no transmission if there are no susceptible people).
286 These hypotheses raise important questions about how to reconcile and ground truth theoretical
287 and empirical studies with field data.

288 The 2015 to 2017 Zika outbreak provided an opportunity to investigate how population
289 and climate affect epidemic dynamics over time and space in a previously unexposed population.
290 The results provide valuable insight into where Zika is likely to become endemic and how future
291 outbreaks transmitted by *Aedes aegypti* could spread. Specifically, given that provinces with

greater populations in their largest cities were associated with longer and more intense outbreaks, regions with larger urban population sizes that also have suitable climate conditions for most of the year are most likely to sustain endemic Zika transmission. However, it is important to carefully consider how these results could apply to other regions, especially in places where Zika may be transmitted by other mosquito species, such as *Aedes africanus*, which exhibit different responses to climate [59]. Zika epidemics in Latin America were characteristically different across countries: some regions experienced large epidemics that spread quickly while others experienced low levels of sustained transmission, and these differences were largely driven by rainfall, mean temperature, and temperature range. We would expect similar epidemic metrics to characterize other mosquito transmitted diseases that could emerge and re-emerge in the future, such as o'nyong nyong, Mayaro, and yellow fever [1,20,41–43]. Given this climate-driven geographic variation in epidemics, we would expect climate change to alter patterns in transmission for emerging and re-remerging mosquito-borne diseases in the future.

Author contributions: EAM and JMC conceived of project; MH acquired data and conducted analyses; MH, JMC, and EAM interpreted data and wrote the manuscript.

Competing interests: All authors declare that there are no competing interests.

Funding: We received funding from a National Science Foundation (NSF) Ecology and Evolution of Infectious Diseases grant (DEB-1518681) and a Research Experiences for Undergraduates supplement, an NSF Grants for Rapid Response Research grant (RAPID 1640780), the Stanford University Woods Institute for the Environment Environmental Ventures Program, and the Hellman Faculty Fellowship.

337 References:

338 1. Gould E, Pettersson J, Higgs S, Charrel R, de Lamballerie X. 2017 Emerging arboviruses:
339 Why today? *One Heal.* **4**, 1–13. (doi:10.1016/j.onehlt.2017.06.001)

340 2. Perkins TA, Metcalf CJE, Grenfell BT, Tatem AJ. 2015 Estimating Drivers of
341 Autochthonous Transmission of Chikungunya Virus in its Invasion of the Americas. *PLoS*
342 *Curr.* (doi:10.1371/currents.outbreaks.a4c7b6ac10e0420b1788c9767946d1fc)

343 3. Fritzell C, Rousset D, Adde A, Kazanji M, Van Kerkhove MD, Flamand C. 2018 Current
344 challenges and implications for dengue, chikungunya and Zika seroprevalence studies
345 worldwide: A scoping review. *PLoS Negl. Trop. Dis.* **12**, 1–29.

346 4. Ali S *et al.* 2017 Environmental and Social Change Drive the Explosive Emergence of
347 Zika Virus in the Americas. *PLoS Negl. Trop. Dis.* **11**, e0005135.
348 (doi:10.1371/journal.pntd.0005135)

349 5. Pan American Health Organization / World Health Organization. 2018 Zika suspected and
350 confirmed cases reported by countries and territories in the Americas: Cumulative cases,
351 2015-2017. Updated as of 04 January 2018.

352 6. Finkenstädt BF, Grenfell BT. 2000 Time series modelling of childhood diseases: a
353 dynamical systems approach. *J. R. Stat. Soc. Ser. C (Applied Stat.* **49**, 187.

354 7. Staples JE, Breiman RF, Powers AM. 2009 Chikungunya Fever: An Epidemiological
355 Review of a Re-Emerging Infectious Disease. *Clin. Infect. Dis.* **49**, 942–948.
356 (doi:10.1086/605496)

357 8. Lardeux FJ, Tejerina RH, Quispe V, Chavez TK. 2008 A physiological time analysis of
358 the duration of the gonotrophic cycle of Anopheles pseudopunctipennis and its
359 implications for malaria transmission in Bolivia. *Malar. J.* **7**, 141. (doi:10.1186/1475-

2875-7-141)

9. Mordecai EAEA *et al.* 2013 Optimal temperature for malaria transmission is dramatically lower than previously predicted. *Ecol. Lett.* **16**, 22–30. (doi:10.1111/ele.12015)

10. Grenfell BT, Bjorndstad ON, Kappey J. 2001 Travelling waves and spatial hierarchies in measles epidemics. *Nature* **414**, 716.

11. Reiner RC *et al.* 2014 Time-varying, serotype-specific force of infection of dengue virus. *Proc. Natl. Acad. Sci.* **111**, E2694–E2702. (doi:10.1073/PNAS.1314933111)

12. French MD *et al.* 2015 Estimation of changes in the force of infection for intestinal and urogenital schistosomiasis in countries with schistosomiasis control initiative-assisted programmes. *Parasit. Vectors* **8**, 558. (doi:10.1186/s13071-015-1138-1)

13. Hafeez S, Amin M, Munir BA. 2017 Spatial mapping of temporal risk to improve prevention measures: A case study of dengue epidemic in Lahore. *Spat. Spatiotemporal. Epidemiol.* **21**, 77–85.

14. Mueller I *et al.* 2012 Force of infection is key to understanding the epidemiology of Plasmodium falciparum malaria in Papua New Guinean children. *Proc. Natl. Acad. Sci. United States Am. VO - 109* , 10030.

15. Pomeroy LW, Bjørnstad ON, Kim H, Jumbo SD, Abdoulkadiri S, Garabed R. 2015 Serotype-Specific Transmission and Waning Immunity of Endemic Foot-and-Mouth Disease Virus in Cameroon. *PLoS One* **10**, e0136642. (doi:10.1371/journal.pone.0136642)

16. Carran S, Ferrari M, Reluga T. 2018 Unintended consequences and the paradox of control: Management of emerging pathogens with age-specific virulence. *PLoS Negl. Trop. Dis.* **12**, e0005997. (doi:10.1371/journal.pntd.0005997)

17. Egger JR, Ooi EE, Kelly DW, Woolhouse ME, Davies CR, Coleman PG. 2008

Reconstructing historical changes in the force of infection of dengue fever in Singapore: implications for surveillance and control. *Bull. World Heal. Organ. VO - 86* , 187.

18. Gardner LM, Bóta A, Gangavarapu K, Kraemer MUG, Grubaugh ND. 2018 Inferring the risk factors behind the geographical spread and transmission of Zika in the Americas. *PLoS Negl. Trop. Dis.* **12**, 1–25.

19. Ali S *et al.* 2017 Environmental and Social Change Drive the Explosive Emergence of Zika Virus in the Americas. *PLoS Negl. Trop. Dis.* **11**, e0005135. (doi:10.1371/journal.pntd.0005135)

20. Nah K, Mizumoto K, Miyamatsu Y, Yasuda Y, Kinoshita R, Nishiura H. 2016 Estimating risks of importation and local transmission of Zika virus infection. *PeerJ* **4**, e1904. (doi:10.7717/peerj.1904)

21. Mordecai EA *et al.* 2017 Detecting the impact of temperature on transmission of Zika, dengue, and chikungunya using mechanistic models. , 1–19.

22. Marcondes CB, Ximenes M de FF de M. 2015 Zika virus in Brazil and the danger of infestation by Aedes (Stegomyia) mosquitoes. *Rev. Soc. Bras. Med. Trop.* **49**, 4–10. (doi:10.1590/0037-8682-0220-2015)

23. Ryan SJ, McNally A, Johnson LR, Mordecai EA, Ben-Horin T, Paaijmans K, Lafferty KD. 2015 Mapping Physiological Suitability Limits for Malaria in Africa Under Climate Change. *Vector Borne Zoonotic Dis.* **15**, 718–25. (doi:10.1089/vbz.2015.1822)

24. Costa EAP de A, Santos EM de M, Correia JC, Albuquerque CMR de. 2010 Impact of small variations in temperature and humidity on the reproductive activity and survival of *Aedes aegypt*i (Diptera, Culicidae). *Rev. Bras. Entomol.* **54**, 488–493. (doi:10.1590/S0085-56262010000300021)

406 25. Delatte H, Gimonneau G, Triboire A, Fontenille D. 2009 Influence of Temperature on
407 Immature Development, Survival, Longevity, Fecundity, and Gonotrophic Cycles of
408 *Aedes albopictus*, Vector of Chikungunya and Dengue in the Indian Ocean. *J. Med.*
409 *Entomol.* **46**, 33–41. (doi:10.1603/033.046.0105)
410 26. Tesla B, Demakovsky LR, Mordecai EA, Ryan SJ, Bonds MH, Ngonghala CN, Brindley
411 MA, Murdock CC. 2018 Temperature drives Zika virus transmission: evidence from
412 empirical and mathematical models. *Proc. R. Soc. B Biol. Sci.* **285**, 20180795.
413 (doi:10.1098/rspb.2018.0795)
414 27. Eling W, Hooghof J, van de Vegte-Bolmer M, Sauerwein R, van Gemert G-J. 2001
415 Tropical temperatures can inhibit development of the human malaria parasite *Plasmodium*
416 *falciparum* in the mosquito. *Proc. Exper. Appl. Entomol* **12**, 151–156.
417 28. Ciota AT, Matacchiero AC, Kilpatrick AM, Kramer LD. 2014 The effect of temperature
418 on life history traits of *Culex* mosquitoes. *J. Med. Entomol.* **51**, 55–62.
419 (doi:10.1603/ME13003)
420 29. Xiao F-Z, Zhang Y, Deng Y-Q, He S, Xie H-G, Zhou X-N, Yan Y-S. 2014 The effect of
421 temperature on the extrinsic incubation period and infection rate of dengue virus serotype
422 2 infection in Aedes albopictus. *Arch. Virol.* **159**, 3053–3057. (doi:10.1007/s00705-014-
423 2051-1)
424 30. Brady OJ *et al.* 2014 Global temperature constraints on Aedes aegypti and Ae. albopictus
425 persistence and competence for dengue virus transmission. *Parasit. Vectors* **7**, 338.
426 (doi:10.1186/1756-3305-7-338)
427 31. Mordecai EA *et al.* 2017 Detecting the impact of temperature on transmission of Zika,
428 dengue, and chikungunya using mechanistic models. *PLoS Negl. Trop. Dis.* **11**, e0005568.

429 (doi:10.1371/journal.pntd.0005568)
430 32. Barton PS, Aberton JG, Kay BH. 2004 Spatial and temporal definition of *Ochlerotatus*
431 *camptorhynchus* (Thomson) (Diptera: Culicidae) in the Gippsland Lakes system of eastern
432 Victoria. *Aust. J. Entomol.* **43**, 16–22. (doi:10.1111/j.1440-6055.2004.00405.x)
433 33. Li CF, Lim TW, Han LL, Fang R. 1985 Rainfall, abundance of Aedes aegypti and dengue
434 infection in Selangor, Malaysia. *Southeast Asian J. Trop. Med. Public Health* **16**, 560–8.
435 34. Stewart-ibarra AM, Lowe R. 2013 Climate and Non-Climate Drivers of Dengue
436 Epidemics in Southern Coastal Ecuador. **88**, 971–981. (doi:10.4269/ajtmh.12-0478)
437 35. Morin CW, Monaghan AJ, Hayden MH, Barrera R, Ernst K. 2015 Meteorologically
438 Driven Simulations of Dengue Epidemics in San Juan, PR. *PLoS Negl. Trop. Dis.* **9**,
439 e0004002. (doi:10.1371/journal.pntd.0004002)
440 36. Riou J, Poletto C, Boëlle P-Y. 2017 A comparative analysis of Chikungunya and Zika
441 transmission. *Epidemics* **19**, 43–52. (doi:10.1016/j.epidem.2017.01.001)
442 37. Anyamba A *et al.* 2012 Climate Teleconnections and Recent Patterns of Human and
443 Animal Disease Outbreaks. *PLoS Negl. Trop. Dis.* **6**, e1465.
444 (doi:10.1371/journal.pntd.0001465)
445 38. Pontes RJ, Spielman A, Oliveira-Lima JW, Hodgson JC, Freeman J. 2000 Vector densities
446 that potentiate dengue outbreaks in a Brazilian city. *Am. J. Trop. Med. Hyg.* **62**, 378–383.
447 (doi:10.4269/ajtmh.2000.62.378)
448 39. Paaijmans KP, Wandago MO, Githeko AK, Takken W, Vulule J. 2007 Unexpected High
449 Losses of Anopheles gambiae Larvae Due to Rainfall. *PLoS One* **2**, e1146.
450 (doi:10.1371/journal.pone.0001146)
451 40. Koenraadt CJM, Harrington LC. 2008 Flushing effect of rain on container-inhabiting

452 mosquitoes *Aedes aegypti* and *Culex pipiens* (Diptera: Culicidae). *J. Med. Entomol.* **45**,
453 28–35. (doi:10.1603/0022-2585(2008)45[28:FEOROC]2.0.CO;2)
454 41. Wilder-Smith A, Gubler DJ, Weaver SC, Monath TP, Heymann DL, Scott TW. 2017
455 Epidemic arboviral diseases: priorities for research and public health. *Lancet. Infect. Dis.*
456 **17**, e101–e106. (doi:10.1016/S1473-3099(16)30518-7)
457 42. LaBeaud AD *et al.* 2015 High rates of o'nyong nyong and Chikungunya virus
458 transmission in coastal Kenya. *PLoS Negl. Trop. Dis.* **9**, e0003436.
459 (doi:10.1371/journal.pntd.0003436)
460 43. Wilder-Smith A, Monath TP. 2017 Responding to the threat of urban yellow fever
461 outbreaks. *Lancet. Infect. Dis.* **17**, 248–250. (doi:10.1016/S1473-3099(16)30588-6)
462 44. CDC Epidemic Prediction Initiative. In press. Zika Data Repository.
463 (doi:10.5281/zenodo.584136)
464 45. The Weather Company. In press. Weather Underground. See
465 https://www.wunderground.com/.
466 46. Stewart Ibarra AM, Ryan SJ, Beltrán E, Mejía R, Silva M, Muñoz Á. 2013 Dengue Vector
467 Dynamics (Aedes aegypti) Influenced by Climate and Social Factors in Ecuador:
468 Implications for Targeted Control. *PLoS One* **8**, e78263.
469 (doi:10.1371/journal.pone.0078263)
470 47. Gharbi M, Quenel P, Gustave J, Cassadou S, La Ruche G, Girdary L, Marrama L. 2011
471 Time series analysis of dengue incidence in Guadeloupe, French West Indies: forecasting
472 models using climate variables as predictors. *BMC Infect. Dis.* **11**, 166.
473 (doi:10.1186/1471-2334-11-166)
474 48. Johansson MA, Dominici F, Glass GE. 2009 Local and Global Effects of Climate on

475 Dengue Transmission in Puerto Rico. *PLoS Negl. Trop. Dis.* **3**, e382.
476 (doi:10.1371/journal.pntd.0000382)
477 49. Laureano-Rosario AE, Garcia-Rejon JE, Gomez-Carro S, Farfan-Ale JA, Muller-Karger
478 FE. 2017 Modelling dengue fever risk in the State of Yucatan, Mexico using regional-
479 scale satellite-derived sea surface temperature. *Acta Trop.* **172**, 50–57.
480 (doi:10.1016/j.actatropica.2017.04.017)
481 50. Brinkhoff T. In press. City Population.
482 51. Johansson MA, Powers AM, Pesik N, Cohen NJ, Staples JE. 2014 Nowcasting the spread
483 of chikungunya virus in the Americas. *PLoS One* **9**, e104915.
484 (doi:10.1371/journal.pone.0104915)
485 52. Faria NR *et al.* 2017 Establishment and cryptic transmission of Zika virus in Brazil and
486 the Americas. *Nature* **546**, 406–410.
487 53. Nakagawa S, Schielzeth H. 2012 A general and simple method for obtaining R2 from
488 generalized linear mixed-effects models. *Methods Ecol. Evol.* **4**, 133–142.
489 (doi:10.1111/j.2041-210x.2012.00261.x)
490 54. Cragg JG, Uhler RS. 1970 The Demand for Automobiles. *Can. J. Econ. / Rev. Can.*
491 *d'Economique* **3**, 386–406. (doi:10.2307/133656)
492 55. NAGELKERKE NJD. 1991 A note on a general definition of the coefficient of
493 determination. *Biometrika* **78**, 691–692. (doi:10.1093/biomet/78.3.691)
494 56. Gething PW, Smith DL, Patil AP, Tatem AJ, Snow RW, Hay SI. 2010 Climate change
495 and the global malaria recession. *Nature* **465**, 342–345. (doi:10.1038/nature09098)
496 57. Wen J, Elong Ngono A, Regla-Nava JA, Kim K, Gorman MJ, Diamond MS, Shresta S.
497 2017 Dengue virus-reactive CD8+ T cells mediate cross-protection against subsequent

498 Zika virus challenge. *Nat. Commun.* **8**, 1459. (doi:10.1038/s41467-017-01669-z)
499 58. Huber JH, Childs ML, Caldwell JM, Mordecai EA. 2018 Seasonal temperature variation
500 influences climate suitability for dengue, chikungunya, and Zika transmission. *PLoS Negl.*
501 *Trop. Dis.* **12**, e0006451. (doi:10.1371/journal.pntd.0006451)
502 59. Vorou R. 2016 Zika virus, vectors, reservoirs, amplifying hosts, and their potential to
503 spread worldwide: what we know and what we should investigate urgently. *Int. J. Infect.*
504 *Dis.* **48**, 85–90. (doi:https://doi.org/10.1016/j.ijid.2016.05.014)
505
506
507
508
509
510
511
512
513
514
515
516
517
518
519
520

Table 1: Province-level epidemic metrics used as response variables in the spatial models.

Force of infection is represented as β_t.

Name	Description
Local Transmission	Binary indicator of whether β_t exceeded one for any week
Max(β)	Maximum value for β_t in weeks β_t exceeded one
Avg(β)	Average value for β_t in weeks β_t exceeded one
Cumulative Cases	Total number of cases reported
Average Weekly Cases	Average number of cases in weeks with any cases reported

Table 2: Coefficients for the presence and intensity of Zika from the spatiotemporal hurdle model. A) Coefficients for the logistic regression model predicting the probability of the presence or absence of local transmission. B) Coefficients for the linear regression model predicting force of infection intensity (β_t). We calculated humidity, mean temperature, and temperature range (difference between the maximum and minimum temperatures observed) over a three-week period, lagged by six weeks from the week of case reporting and cumulative rainfall over a six-week period, lagged by three weeks from the week of case reporting.

A: Presence/Absence, $P(\beta_t > 1)$

Term	Estimate	Standard Error	Z-value	p-value
Humidity	0.288	0.071	4.041	$5.32 * 10^{-5}$
Maximum Temperature	0.542	0.087	6.192	$5.96 * 10^{-10}$

B: Intensity Given Presence, β_t

Term	Estimate	Standard Error	t-value	p-value
Rainfall	0.064	0.029	2.216	$2.69 * 10^{-2}$
Average Temperature^2	-0.185	0.060	-3.087	$2.07 * 10^{-3}$
Range	-0.137	0.040	-3.419	$6.49 * 10^{-4}$

Figure 1: Depiction of epidemic metrics that characterize the presence, burden, and intensity of outbreaks. A) cartoon of weekly incidence during an outbreak where cumulative cases are calculated by taking the sum of all cases across all weeks during the outbreak, and average cases (dashed horizontal line) are calculated as the average of all cases in weeks with at least one case during the outbreak. B) cartoon of weekly force of infection during an outbreak where local transmission is calculated as one if β_t exceeded one for any weeks within a province and 0 otherwise. The maximum and average values for β_t are calculated across weeks when β_t exceeded one.

Figure 2: Time series of weekly case incidence and force of infection. Each row corresponds to a single province over time, with lines separating the following countries: DOM = Dominican Republic, SLV = El Salvador, COL = Colombia, ECU = Ecuador, MEX = Mexico, GTM = Guatemala. Gray shading indicates no reporting. A) weekly case incidence The color represents cumulative cases (upper) and log(β_t) (lower) scaled within each province. Red indicates high values and yellow indicates low values. White indicates no cases reported (A) or no local transmission B; (β_t<1) in a given week.

Figure 3: Geographic differences in epidemic metrics. Provinces are colored by A) whether local Zika transmission was present (red) or absent (green); and B) average force of infection (β_t). Provinces that we excluded from this study due to lack of epidemiological or climate data (see methods) are white. Countries not included in this study are grey.

Figure 4: Coefficients for factors driving geographic differences in epidemics. Plots display coefficients included in the best fit model for local transmission (pink), maximum β (blue), average β (green), cumulative cases (yellow), and average weekly cases (orange). Dots and horizontal lines indicate the coefficient values and 95% confidence intervals respectively. A) coefficients for climate and population covariates. B) coefficients for country fixed effects.

Figure 5: Zika intensity peaked in locations with average temperatures of 24°C. Partial residual plot shows the relationship between average mean temperature and average β_t in provinces with local transmission. Observations for all provinces in study (black points) show the variation around the model predicted relationship (red line).

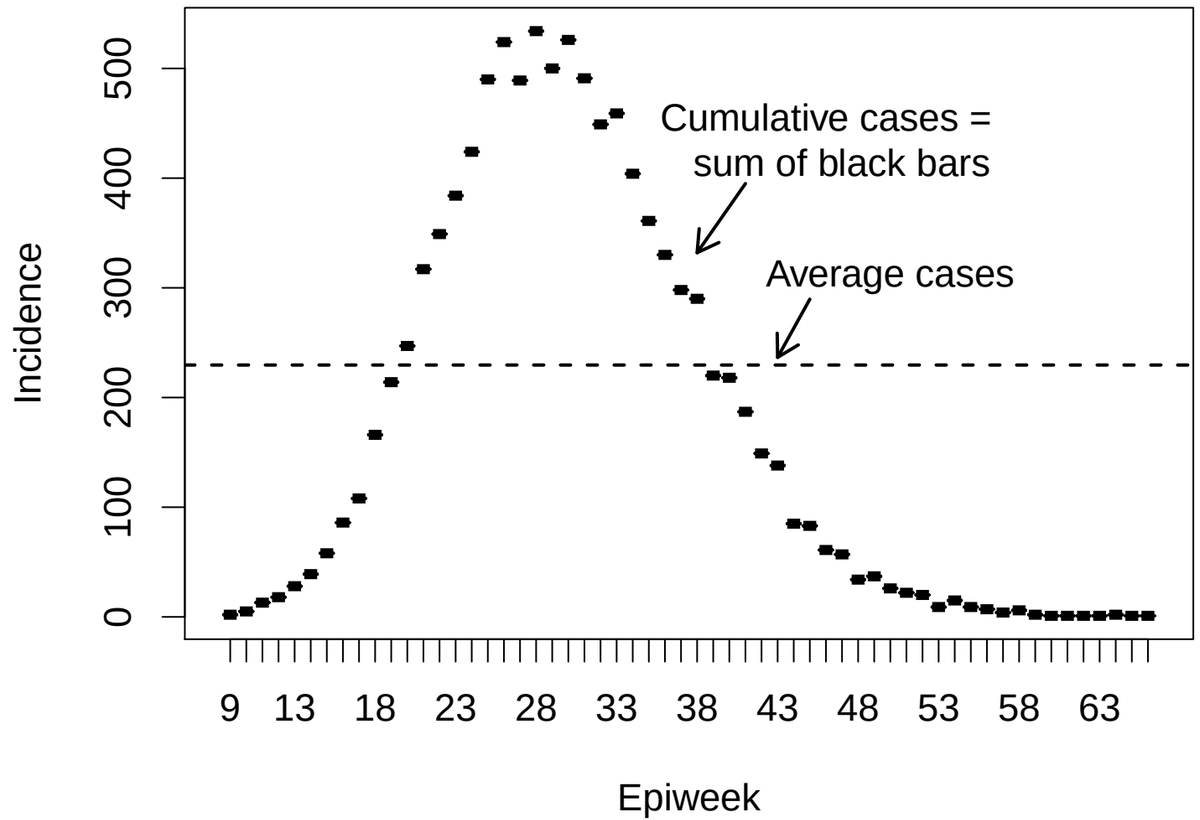
Incidence
0
100
200
300
400
500
Cumulative cases =
sum of black bars
Average cases
9
13
18
23
28
33
38
43
48
53
58
63
Epiweek

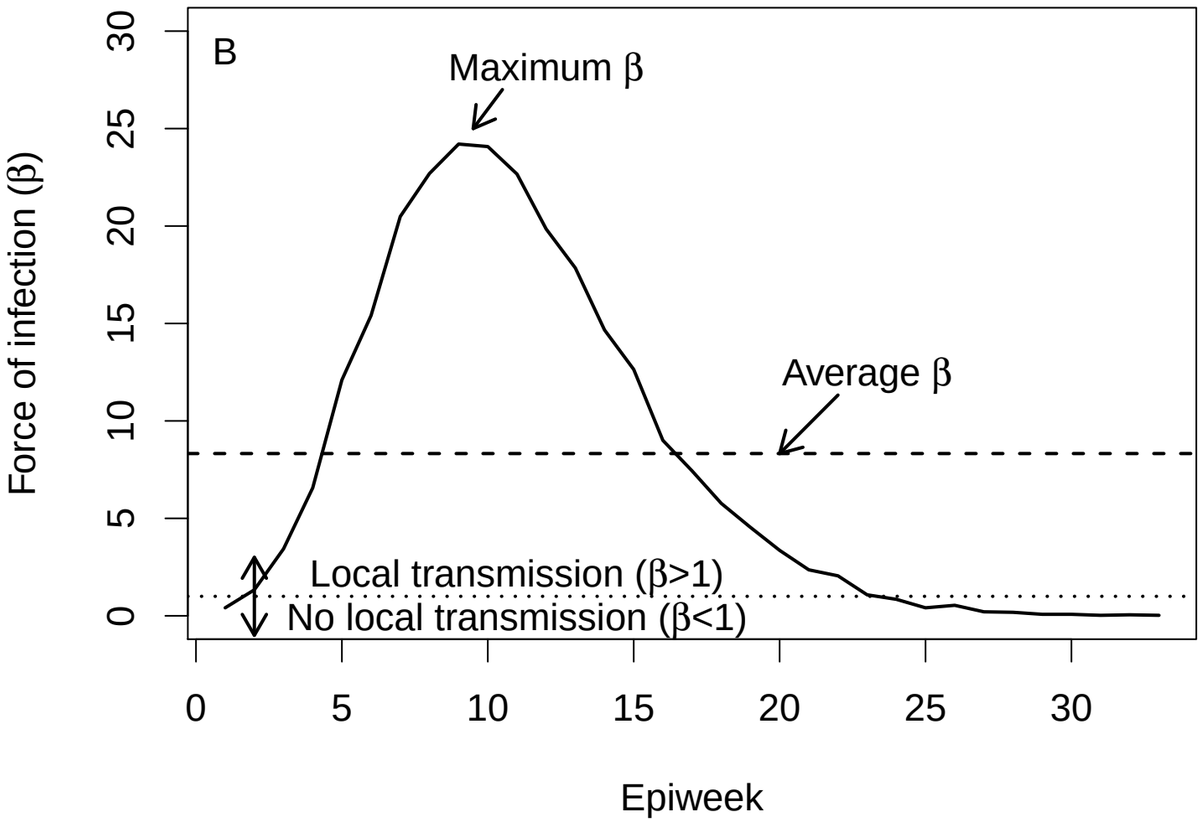
B
Force of infection (β)
0
5
10
15
20
25
30
Maximum β
Average β
Local transmission (β>1)
No local transmission (β<1)
0
5
10
15
20
25
30
Epiweek

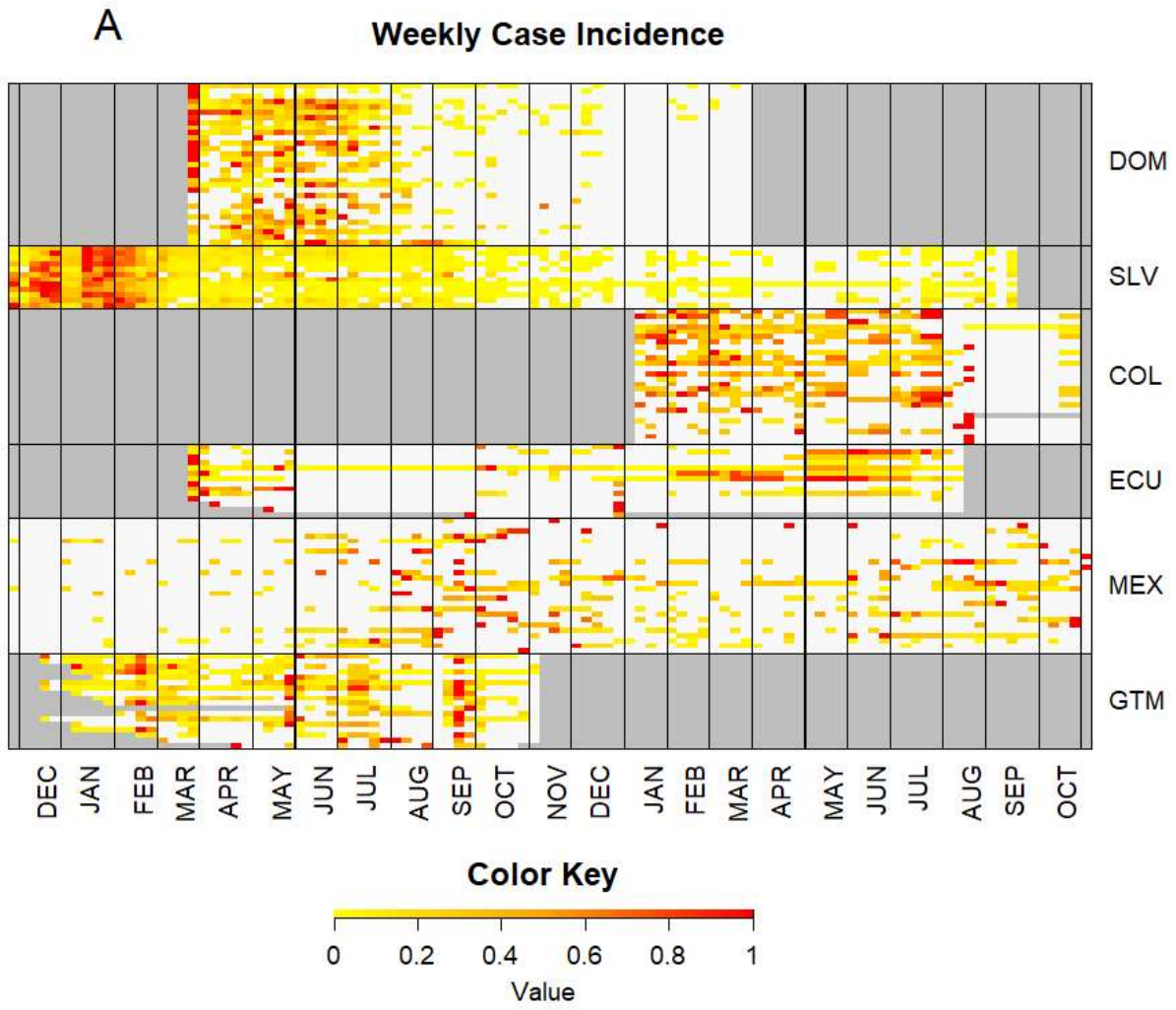
A
Weekly Case Incidence
DOM
SLV
COL
ECU
MEX
GTM
DEC
JAN
FEB
MAR
APR
MAY
JUN
JUL
AUG
SEP
OCT
NOV
DEC
JAN
FEB
MAR
APR
MAY
JUN
JUL
AUG
SEP
OCT
Color Key
0
0.2
0.4
0.6
0.8
1
Value

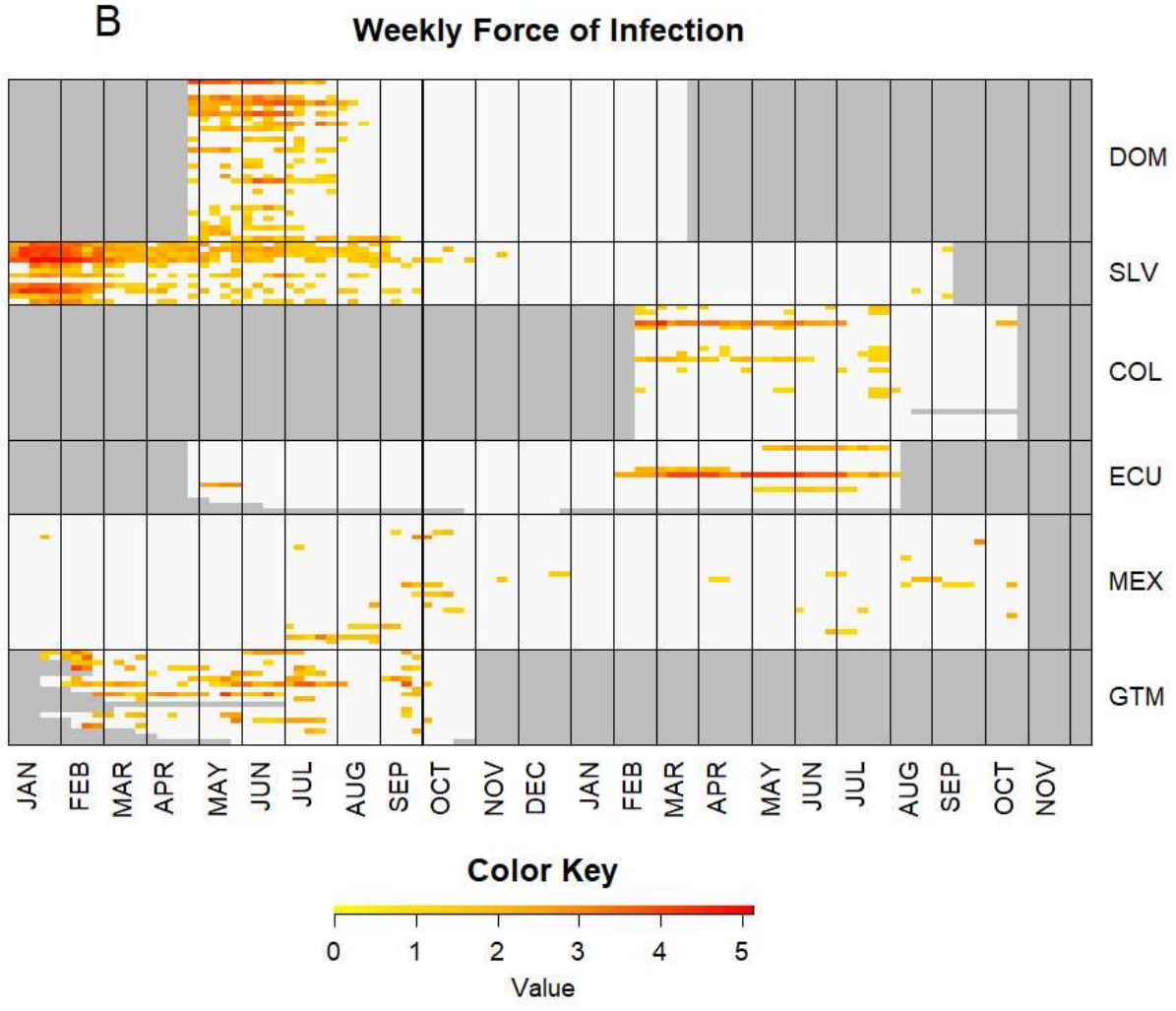
B
Weekly Force of Infection
DOM
SLV
COL
ECU
MEX
GTM
JAN
FEB
MAR
APR
MAY
JUN
JUL
AUG
SEP
OCT
NOV
DEC
JAN
FEB
MAR
APR
MAY
JUN
JUL
AUG
SEP
OCT
NOV
Color Key
0
1
2
3
4
5
Value

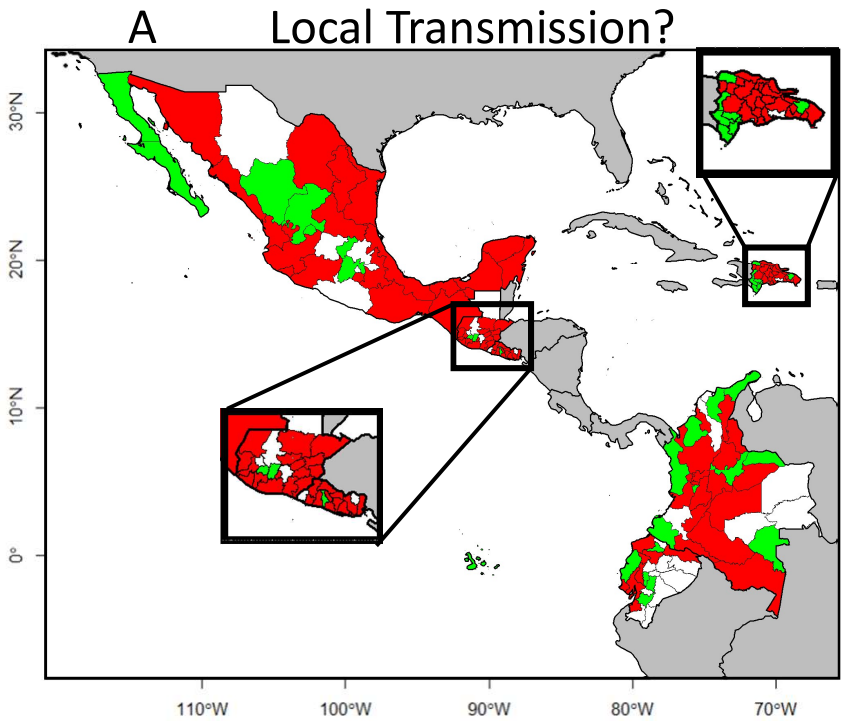
A
Local Transmission?
30°N
20°N
10°N
0°
110°W
100°W
90°W
80°W
70°W

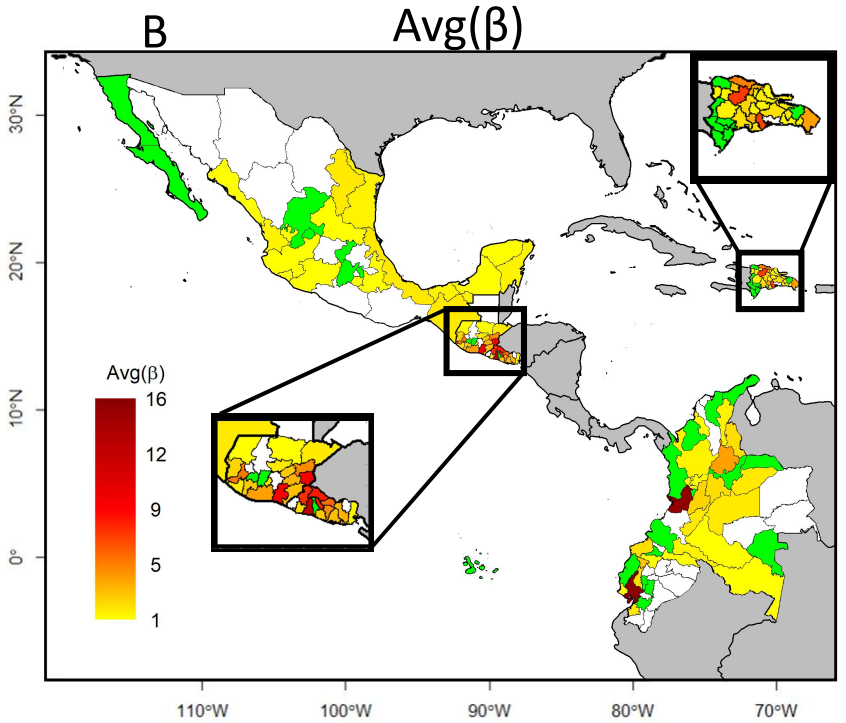
B
Avg(β)
Avg(β)
16
12
9
5
1
30°N
20°N
10°N
0°
110°W
100°W
90°W
80°W
70°W

A

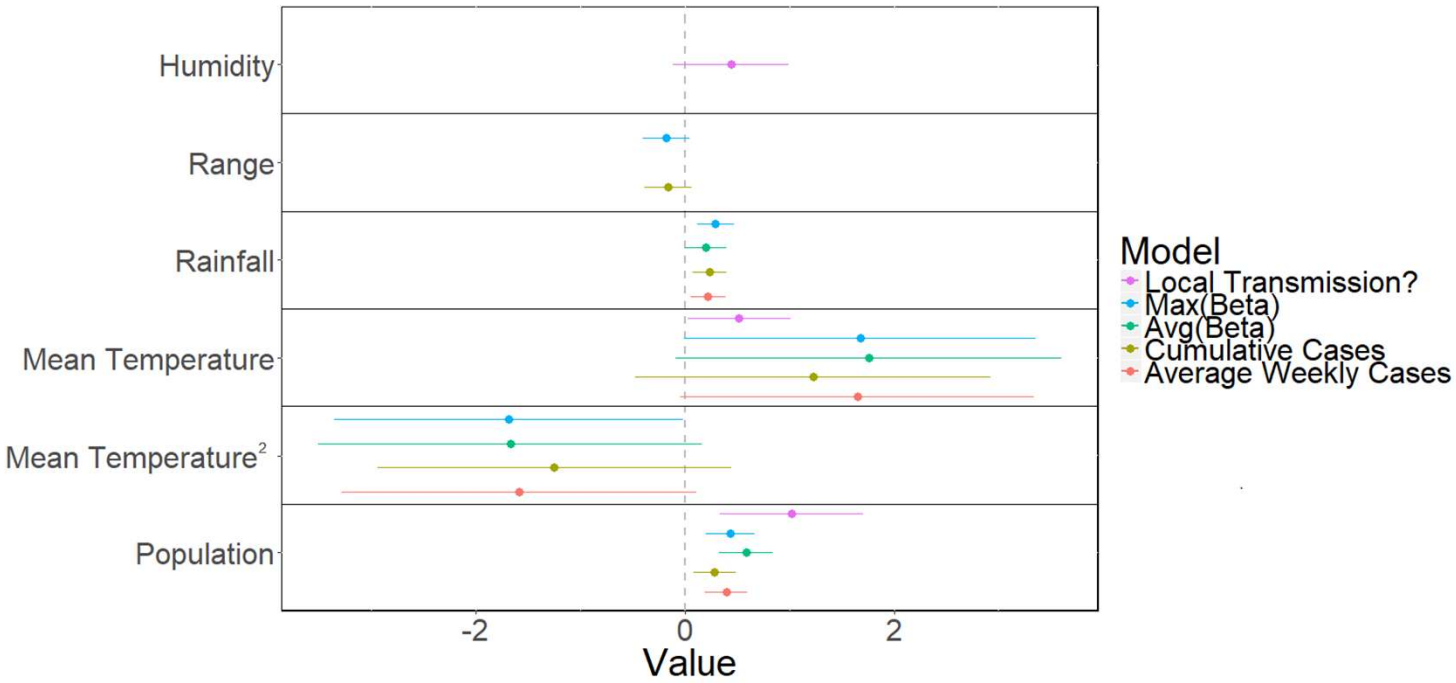
Humidity
Range
Rainfall
Mean Temperature
Mean Temperature²
Population
-2
0
2
Value
Model
Local Transmission?
Max(Beta)
Avg(Beta)
Cumulative Cases
Average Weekly Cases

B

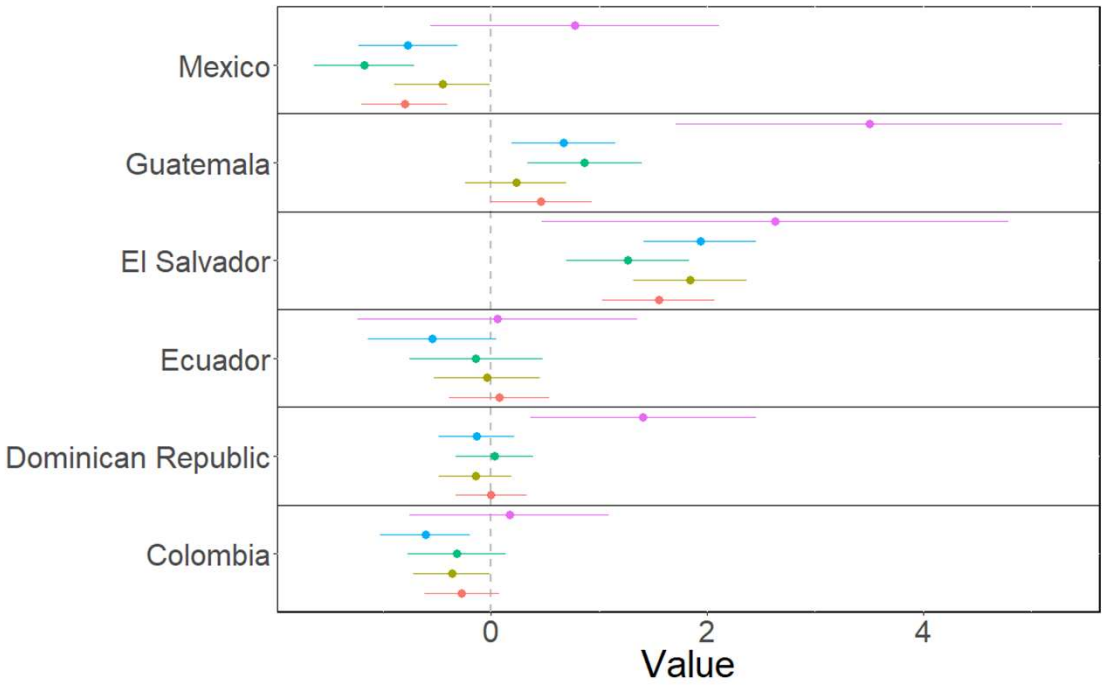
Mexico
Guatemala
El Salvador
Ecuador
Dominican Republic
Colombia
0
2
4
Value

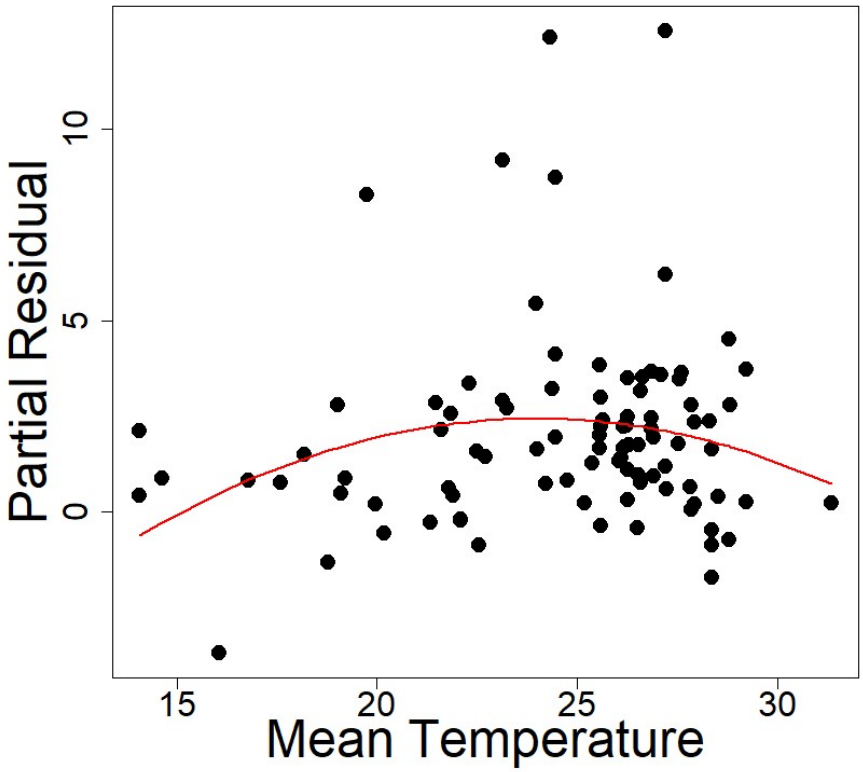
Partial Residual
0
5
10
15
20
25
30
Mean Temperature